Research Article | Vol. 25, No. 19 | 18 Sep 2017 | OPTICS EXPRESS 23035
Optics EXPRESS

Efficient second harmonic generation in low-loss planar GaN waveguides

MAKSYM GROMOVYI,[1,*] JULIEN BRAULT,[1] AIMERIC COURVILLE,[1], STÉPHANIE RENNESSON,[1] FABRICE SEMOND,[1] GUY FEUILLET, [4] PASCAL BALDI,[2] PHILIPPE BOUCAUD,[3] JEAN-YVES DUBOZ,[1] AND MARC P. DE MICHELI[2]

[1] *Université Côte d'Azur, CNRS, CRHEA, rue Bernard Grégory, 06560 Valbonne, France*
[2] *Université Côte d'Azur, CNRS, INΦNI, Parc Valrose, 06100 Nice, France*
[3] *Centre de Nanosciences et de Nanotechnologies, CNRS, Univ. Paris-Sud, Université Paris-Saclay, Bâtiment 220, Rue André Ampère, F-91405 Orsay, France*
[4] *Université Grenoble Alpes, CEA, LETI, MINATEC Campus, F-38054 Grenoble, France*
[*] *Maksym.Gromovyi@crhea.cnrs.fr*

Abstract: We demonstrate low-loss GaN/AlGaN planar waveguides grown by molecular beam epitaxy on sapphire substrates. By using a proper AlGaN cladding layer and reducing surface roughness we reach <1dB/cm propagation losses at 633nm. These low propagation losses allow an efficient second harmonic generation using modal phase matching between a TM0 pump at 1260nm and a TM2 second harmonic at 630nm. A maximal power conversion of 2% is realized with an efficiency of $0.15\%\cdot W^{-1}cm^{-2}$. We provide a modelling that demonstrates broadband features of GaN/AlGaN platform by showing second harmonic wavelengths tunability from the visible up to the near-infrared spectral region. We discuss drawbacks of modal phase matching and propose a novel solution which allows a drastic improvement of modal overlaps with the help of a planar polarity inversion. This new approach is compatible with low propagation losses and may allow as high as $100\%\cdot W^{-1}cm^{-2}$ conversion efficiencies in the future.

OCIS codes: (190.2620) Harmonic generation and mixing; (190.4390) Nonlinear optics, integrated optics.

References and links

1. J. Miragliotta, D. K. Wickenden, T. J. Kistenmacher, and W. A. Bryden, "Linear- and nonlinear-optical properties of GaN thin films," J. Opt. Soc. Am. B **10**(8), 1447–1456 (1993).
2. N. A. Sanford, A. V. Davydov, D. V. Tsvetkov, A. V. Dmitriev, S. Keller, U. K. Mishra, S. P. Denbaars, S. S. Park, J. Y. Han, and R. J. Molnar, "Measurement of second order susceptibilities of GaN and AlGaN," J. Appl. Phys. **97**(5), 053512 (2005).
3. A. W. Bruch, C. Xiong, B. Leung, M. Poot, J. Han, and H. X. Tang, "Broadband nanophotonic waveguides and resonators based on epitaxial GaN thin films," Appl. Phys. Lett. **107**(14), 141113 (2015).
4. I. Roland, Y. Zeng, X. Checoury, M. El Kurdi, S. Sauvage, C. Brimont, T. Guillet, B. Gayral, M. Gromovyi, J. Y. Duboz, F. Semond, M. P. de Micheli, and P. Boucaud, "Near-infrared III-nitride-on-silicon nanophotonic platform with microdisk resonators," Opt. Express **24**(9), 9602–9610 (2016).
5. Y. Zeng, I. Roland, X. Checoury, Z. Han, M. El Kurdi, S. Sauvage, B. Gayral, C. Brimont, T. Guillet, M. Mexis, F. Semond, and P. Boucaud, "Resonant second harmonic generation in a gallium nitride two-dimensional photonic crystal on silicon," Appl. Phys. Lett. **106**(8), 081105 (2015).
6. Y. Zeng, I. Roland, X. Checoury, Z. Han, M. El Kurdi, S. Sauvage, B. Gayral, C. Brimont, T. Guillet, F. Semond, and P. Boucaud, "Imaging of Photonic Crystal Localized Modes through Third-Harmonic Generation," ACS Photonics **3**(7), 1240–1247 (2016).
7. M. S. Mohamed, A. Simbula, J.-F. Carlin, M. Minkov, D. Gerace, V. Savona, N. Grandjean, M. Galli, and R. Houdré, "Efficient continuous-wave nonlinear frequency conversion in high-Q gallium nitride photonic crystal cavities on silicon," APL Photonics **2**(3), 031301 (2017).
8. M. M. Fejer, G. A. Magel, D. H. Jundt, and R. Byer, "Quasi phase-matching second harmonic generation : tuning and tolerances," IEEE J. Quantum Electron. **28**(11), 2631–2654 (1992).
9. D. S. Hum and M. M. Fejer, "Quasi-phasematching," C. R. Phys. **8**(2), 180–198 (2007).
10. S. Pezzagna, P. Vennéguès, N. Grandjean, A. D. Wieck, and J. Massies, "Submicron periodic poling and chemical patterning of GaN," Appl. Phys. Lett. **87**(6), 062106 (2005).
11. J. Hite, M. Twigg, M. Mastro, J. Freitas, J. Meyer, I. Vurgaftman, S. O'Connor, N. Condon, F. Kub, S. Bowman, and C. Eddy, "Development of periodically oriented gallium nitride for non-linear optics," Opt. Mater. Express **2**(9),

#301925 http://dx.doi.org/10.1364/OE.25.023035
Journal © 2017 Received 7 Jul 2017; revised 20 Aug 2017; accepted 22 Aug 2017; published 12 Sep 2017

Optics EXPRESS

1203–1208 (2012).
12. D. Alden, W. Guo, R. Kirste, F. Kaess, I. Bryan, T. Troha, A. Bagal, P. Reddy, L. H. Hernandez-Balderrama, A. Franke, S. Mita, C. H. Chang, A. Hoffmann, M. Zgonik, R. Collazo, and Z. Sitar, "Fabrication and structural properties of AlN submicron periodic lateral polar structures and waveguides for UV-C applications," Appl. Phys. Lett. **108**(26), 261106 (2016).
13. A. Chowdhury, H. M. Ng, M. Bhardwaj, and N. G. Weimann, "Second-harmonic generation in periodically poled GaN," Appl. Phys. Lett. **83**(6), 1077–1079 (2003).
14. D. N. Hahn, G. T. Kiehne, J. B. Ketterson, G. K. L. Wong, P. Kung, A. Saxler, and M. Razeghi, "Phase-matched optical second-harmonic generation in GaN and AlN slab waveguides," J. Appl. Phys. **85**(5), 2497–2501 (1999).
15. D. Blanc, A. M. Bouchoux, C. Plumereau, A. Cachard, and J. F. Roux, "Phase-matched frequency doubling in an aluminum nitride waveguide with a tunable laser source," Appl. Phys. Lett. **66**(6), 659–661 (1995).
16. I. Roland, M. Gromovyi, Y. Zeng, M. El Kurdi, S. Sauvage, C. Brimont, T. Guillet, B. Gayral, F. Semond, J. Y. Duboz, M. de Micheli, X. Checoury, and P. Boucaud, "Phase-matched second harmonic generation with on-chip GaN-on-Si microdisks," Sci. Rep. **6**, 34191 (2016).
17. C. Xiong, W. H. P. Pernice, K. K. Ryu, C. Schuck, K. Y. Fong, T. Palacios, and H. X. Tang, "Integrated GaN photonic circuits on silicon (100) for second harmonic generation," Opt. Express **19**(11), 10462–10470 (2011).
18. X. Guo, C. Zou, and H. Tang, "Second-harmonic generation in aluminum nitride microrings with 2500 %/ W conversion efficiency," Optica **3**(10), 1126–1131 (2016).
19. O. Westreich, M. Katz, Y. Paltiel, O. Ternyak, and N. Sicron, "Low propagation loss in GaN/AlGaN-based ridge waveguides," Phys. Status Solidi A **212**(5), 1043–1048 (2015).
20. A. Stolz, E. Cho, E. Dogheche, Y. Androussi, D. Troadec, D. Pavlidis, and D. Decoster, "Optical waveguide loss minimized into gallium nitride based structures grown by metal organic vapor phase epitaxy," Appl. Phys. Lett. **98**(16), 161903 (2011).
21. S. Pezzagna, J. Brault, M. Leroux, J. Massies, and M. De Micheli, "Refractive indices and elasto-optic coefficients of GaN studied by optical waveguiding," J. Appl. Phys. **103**(12), 123112 (2008).
22. Ü. Özgür, G. Webb-Wood, H. O. Everitt, F. Yun, and H. Morkoç, "Systematic measurement of $Al_xGa_{1-x}N$ refractive indices," Appl. Phys. Lett. **79**(25), 4103–4105 (2001).
23. N. Grandjean, A. Dussaigne, S. Pezzagna, and P. Vennéguès, "Control of the polarity of GaN films using an Mg adsorption layer," J. Cryst. Growth **251**(1), 460–464 (2003).
24. P. K. Tien and R. Ulrich, "Theory of prism-film coupler and thin-film light guides," J. Opt. Soc. Am. **60**(10), 1325–1327 (1970).
25. S. Vézian, F. Natali, F. Semond, and J. Massies, "From spiral growth to kinetic roughening in molecular-beam epitaxy of GaN(0001)," Phys. Rev. B **69**(12), 125329 (2004).
26. W. H. Pernice, C. Xiong, and H. X. Tang, "High Q micro-ring resonators fabricated from polycrystalline aluminum nitride films for near infrared and visible photonics," Opt. Express **20**(11), 12261–12269 (2012).

1. Introduction

Considerable amount of research in recent years has been focused on GaN as a novel material for nonlinear optics and photonics. GaN is a large band gap semiconductor which is well known for its outstanding optoelectronic properties and numerous applications in domains of light emitting devices, high power and high frequency electronics. It is mainly grown in a form of thin films by metalorganic vapour phase epitaxy (MOVPE) or by molecular beam epitaxy (MBE) on sapphire or silicon substrates. During an epitaxial growth, GaN crystalizes in a wurtzite phase which has inherent second order nonlinear properties due to its noncentro-symmetric crystalline structure.

A unique combination of a direct band gap, a large transparency window and a high second order nonlinearity [1, 2] makes GaN an interesting candidate for nonlinear optics. In addition, GaN films can further be structured to fabricate waveguides, microrings [3], microdiscs [4] and photonic crystals [5–7]. These photonic structures can improve second harmonic generation (SHG), since they provide higher power densities, longer propagation distances and cavity field enhancements. In order to realize an efficient SHG process one also needs to satisfy phase matching conditions and at the same time preserve low propagation losses, which can be a challenging task.

One of the most well known techniques, that allows to satisfy phase matching conditions in waveguides, is quasi-phasematching (QPM) [8, 9]. Several groups, including our group, have been trying to grow periodically oriented GaN structures (PO-GaN) which allow quasi-phasematching [10–13]. However, this approach leads to very high propagation losses, which suppress all the advantages of the achieved phase matching. So far, there were only few reports

Optics EXPRESS

on second harmonic generation in PO-GaN and power conversions for these structure remain very low <0.1% with an efficiency of $1.2 \cdot 10^{-4}\%\cdot W^{-1}cm^{-2}$ [13].

An alternative technique to QPM is modal phase matching (MPM), which was already reported for GaN based planar waveguides [14, 15], micro-disks [16] and miro-rings [17]. The best power conversion of $1.8 \cdot 10^{-3}\%$ was achieved in GaN microrings with an efficiency of $1.5 \cdot 10^{-2}\%\cdot W^{-1}$ [17]. In this case both poor modal overlaps and relatively high propagation losses have contributed to the low conversion efficiency. In the meantime a very high power conversion of 12% was recently reported for AlN micro-rings [18]. Although AlN has a 10 times smaller non-linear coefficient $\chi^{(2)}_{AlN} = 1\,pm/V$ [2, 18] compared to GaN $\chi^{(2)}_{GaN} = 10\,pm/V$ [2], ultra low propagation losses have largely compensated for the small non-linearity [18]. This shows that propagation losses are a key factor and that they limit the performance of GaN based structures. There have been few studies addressing this issue, however the origins of the propagation losses are still unclear and despite the fact that epitaxial GaN layers have a better crystalline quality than sputtered AlN layers, the propagation losses remain quite high, around 1dB/cm in the near-infrared [19] and 10dB/cm in the visible spectral region [20].

As we can see, there has been some partial progress on the problems of phase matching and propagation losses, however low-loss GaN based structures optimized for efficient nonlinear interactions have not been demonstrated so far. Low-loss GaN structures could give a big advantage over corresponding AlN structures, since their 10 times larger non-linear coefficient could provide 100 times higher conversion efficiencies.

In this work we present GaN based waveguides designed for second harmonic generation with very low propagation losses going below 1dB/cm at 633nm. Using these waveguides we were able to reach a power conversion of 2% from the near-infrared to the visible spectral region with an efficiency of $0.15\%\cdot W^{-1}cm^{-2}$, which is, to our best knowledge, the highest value reported so far for GaN waveguides. We demonstrate that by fabricating proper optical cladding layers and reducing surface roughness one can eliminate a large portion of the propagation losses and obtain high quality guiding layers which can be used for further integrated photonic applications.

2. Modal phase matching in GaN/AlGaN waveguides

In this section we present the modal phase matching (MPM) possibilities for waveguides with GaN guiding layers and AlGaN substrates. The GaN on AlGaN configuration is particularly interesting because AlGaN can serve as an optical cladding layer and at the same time this configuration provides a modal dispersion sufficiently high to compensate for the material chromatic dispersion.

In this paragraph all the calculations were done in Mathematica using a standard analytical model for modes confined in planar waveguides. Here we used a three layer model (air/GaN/AlGaN) for planar waveguides and we limited ourselves to a highly confined case (>70% of modal power in GaN), so that AlGaN indeed can be considered as an optical cladding layer. We took into consideration ordinary and extraordinary dispersions for both GaN [21] and AlGaN [22] materials, and the variation of the $\chi^{(2)}$ nonlinear coefficient with the Al content for AlGaN alloys [2]. We assumed that $\chi^{(2)}_{GaN} = 10\,pm/V$, $\chi^{(2)}_{AlN} = 1\,pm/V$, and for AlGaN alloys we used a simple approximation $\chi^{(2)}_{Al_yGa_{1-y}N} = y \cdot \chi^{(2)}_{AlN} + (1-y) \cdot \chi^{(2)}_{GaN}$, which fits very well the data provided in [2]. Here we present second harmonic (SH) wavelengths ranges that can be covered using TM0/TM1 and TM0/TM2 modal phase matchings. In addition, we calculate the efficiencies that can be reached with MPM and show how these efficiencies can be enhanced using improved modal overlaps due to a planar polarity inversion. We also present conversion efficiencies between fundamental modes for PO-GaN structures as a reference solution. All calculations were done for TM-modes, since they allow to use the largest component of the nonlinear coefficient χ_{zzz}.

In Fig. 1(a) we plot the field profiles of the TM modes at 633nm for the waveguide that was

Optics EXPRESS

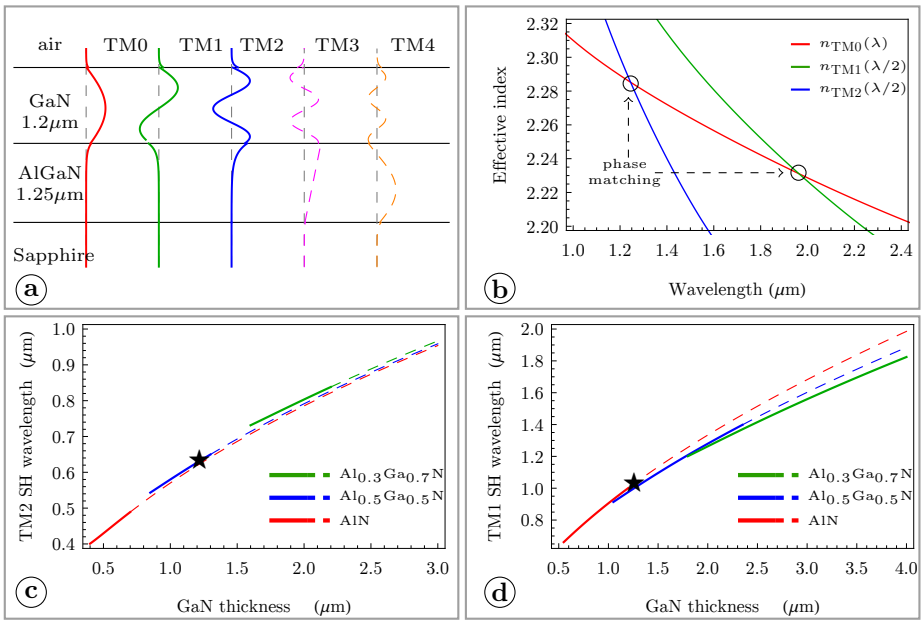

Fig. 1. (a) TM-modes profiles for the fabricated waveguide. (b) Dispersion curves for the effective refractive indices of three guided modes; a modal phase matching (MPM) is reached between TM0 and TM2 modes at 1260nm, and between TM0 and TM1 modes at 1900nm. (c) TM2 second harmonic wavelength as a function of GaN guiding layer thickness for the different AlGaN substrates. (d) TM1 second harmonic wavelength as a function of GaN guiding layer thickness for different AlGaN substrates; the dashed segments of the curves on in Figs. 1(c) and 1(d) indicate a multi-mode nature of waveguides at the wavelength of the pump. The two star symbols in (c) and (d) show how our waveguide fits into this general framework.

fabricated in our work. We studied three main modes TM0, TM1, TM2 that are highly confined in the GaN layer, while the overall GaN/AlGaN/sapphire structure supports multiple higher order modes. Figure 1(b) confirms that for our waveguide the phase matching conditions can be reached at 1260nm and 1900nm, when the effective refractive index of the TM0 pump mode is equal to the effective indices of the TM2 and TM1 second harmonic modes respectively.

In general the phase matching wavelengths depend on the thickness of the GaN guiding layer as well as on the Al content in the AlGaN alloy, as shown in the Figs. 1(c) and 1(d). It should be noted that the phase matching wavelengths strongly depend on the GaN thickness, and are less sensitive to the Al content in the AlGaN alloy. The Al content determines the index contrast and therefore the spectral range that can be covered by SHG, and whether for a given GaN thickness the waveguide will be mono-mode or multi-mode at the pump wavelength. It should be noted that the GaN/AlN configuration allows to cover the broadest spectral range. By summarizing the results presented in the Figs. 1(c) and 1(d) we can conclude that the TM0/TM2 configuration is well suitable for the near-infrared to visible conversion, while the TM0/TM1 case is more adapted for the mid-infrared to near-infrared conversion. The two star symbols in Figs. 1(c) and 1(d) show how our waveguide fits into this general framework.

The main drawback of MPM is the interaction between a fundamental mode and higher order

Optics EXPRESS

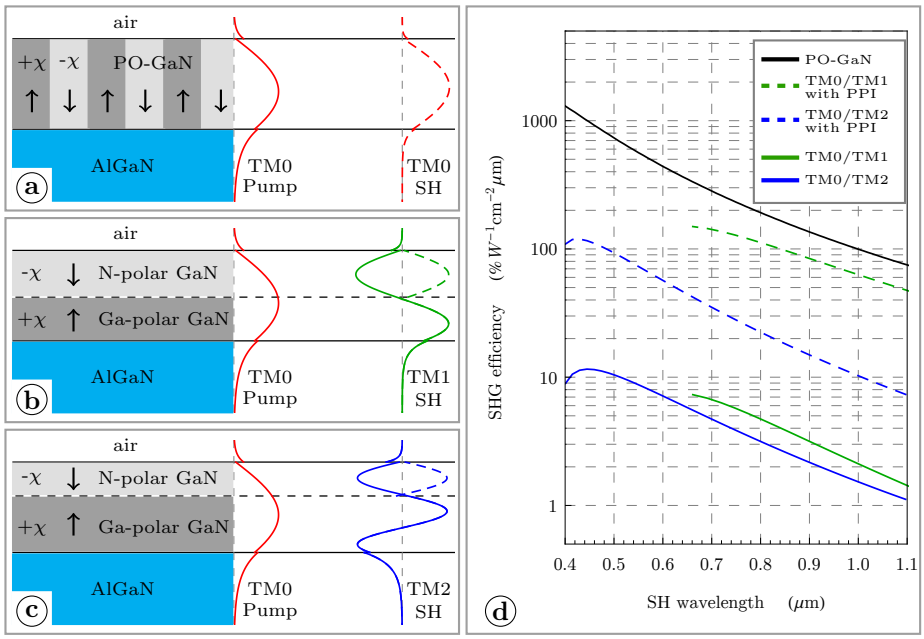

Fig. 2. (a) PO-GaN waveguide allows a power conversion between fundamental modes due to the quasi-phasematching (QPM). In (b) and (c) we show a standard modal phase matching (MPM) technique with an additional improvement of modal overlaps due to the planar polarity inversion (PPI). The plot (d) presents the conversion efficiencies as a function of the harmonic wavelength for the cases of MPM, MPM with an improved overlap and QPM. Efficiencies are given in $\%\cdot\mathrm{W}^{-1}\mathrm{cm}^{-2}\cdot\mu\mathrm{m}$ units and all the calculations are done within the assumption of nondepletion of the pump. In the plot (d) solid black curve represents a reference solution for the case of QPM between TM0-modes in PO-GaN; the green curves corresponds to MPM between TM0 and TM1 modes, while the blue curves corresponds to MPM between TM0 and TM2 modes. In the plot (d) both the blue and green dashed lines give the conversion efficiencies with improved overlaps due to the planar polarity inversion (PPI), while the solid blue and green lines represent a standard MPM with poor modal overlaps.

modes which leads to a poor fields overlap:

$$\text{overlap} = \left(\int_{-\infty}^{+\infty} \chi_{zzz}(z) \mathcal{E}_P^2(z) \mathcal{E}_{SH}(z)\, dz \right)^2, \tag{1}$$

where $\mathcal{E}_P$ and $\mathcal{E}_{SH}$ are the modal field profiles for the pump and the second harmonic respectively, χ_{zzz} is a nonlinear coefficient profile (the z-axis corresponds to the direction of the crystal growth). Indeed, $\mathcal{E}_P^2$ always stays positive, while $\mathcal{E}_{SH}$ changes sign for TM1 and TM2 modes leading to a small value of the integral (1). Fortunately the overlap (1) depends not only on fields profiles, but also on the distribution of the χ_{zzz} nonlinear coefficient along the z axis. As a consequence, there exists a neat solution allowing to improve the modal overlap by using a planar polarity inversion, as schematically shown in the Figs. 2(b) and 2(c). The inversion of the χ_{zzz} sign at the point where TM1 field has its zero value conterbalances the sign change of $\mathcal{E}_{SH}$ drastically increasing the value of the integral (1), see Fig. 2(b). The same approach partially works for the TM2 mode, see Fig. 2(c). This approach is particularly interesting as χ_{zzz} sign is determined by the polarity of GaN and its inversion can be experimentally realized

Optics EXPRESS

for GaN waveguides. One approach consists in reversing the GaN polarity directly during the MBE growth by Mg doping [23]. This method was already used for the fabrication of PO-GaN structures [10]. Another approach consists in bonding of two appropriate Ga-polar GaN layers. It should be noted that wafer bonding has already been used for the fabrication of GaN photonic circuits on SiO_2 substrates [17].

Figure 2(d) summarizes the theoretical efficiencies that can be reached in planar waveguides for the cases of simple modal phase matching, MPM with an improved overlap due to the planar polarity inversion and quasi-phasematching for PO-GaN. All the results are obtained within the assumption of nondepletion of the pump. Since the calculations are done for planar waveguides, we give the efficiencies in $\%\cdot W^{-1}cm^{-2}\cdot\mu m$ units. It means that, for example, to estimate the efficiencies in standard $\%\cdot W^{-1}cm^{-2}$ units for 5μm wide ridge waveguide one needs to divide by 5 all the values given in Fig. 2(d). In theory the highest conversion efficiencies can be reached in PO-GaN waveguides, but so far the performance of these structures was largely compromised by optical losses due to macroscopic surface roughness induced by different growth rates for N- and Ga- polarities. From the Fig. 2(d) we can conclude that MPM with planar polarity inversion can provide an interesting compromise between pure MPM and quasi-phasematching in PO-GaN, since it can provide conversion efficiencies reaching $100\%\cdot W^{-1}cm^{-2}$ in ridge waveguides and at the same time it can eliminate the problem of the high surface roughness present in PO-GaN.

3. Fabrication of low-loss waveguides

In this paragraph we describe the general structure of the planar waveguide that we used for second harmonic generation. We also explain the specific choices that we made during the fabrication in order to reduce the propagation losses. We clearly identify the surface roughness as one of the major sources of the propagation losses and show that an improvement of the surface smoothness is an essential factor for low propagation losses.

The waveguiding heterostructures were grown on (0001) sapphire substrates by molecular beam epitaxy (MBE). Solid sources were used for the III-elements and ammonia (NH3) was employed as the nitrogen precursor. First, a low temperature 30-nm thick GaN buffer layer was deposited followed by a 125-nm thick AlN layer grown at 950 °C. The AlN is used to get a compressive strain when growing the following AlGaN layer and avoid the formation of cracks. Next, a 1μm-thick $Al_{0.65}Ga_{0.35}N$ layer, used as the lower optical cladding layer, was grown at a temperature of 870 °C. Finally, a 1.2 μm thick GaN guiding layer was grown at 800 °C. The sample was then introduced into a MOVPE reactor to grow a 60nm GaN layer at 1080 °C in order to smooth the surface. A cross-sectional scanning electron microscope (SEM) image of the fabricated waveguide is shown in Fig. 3.

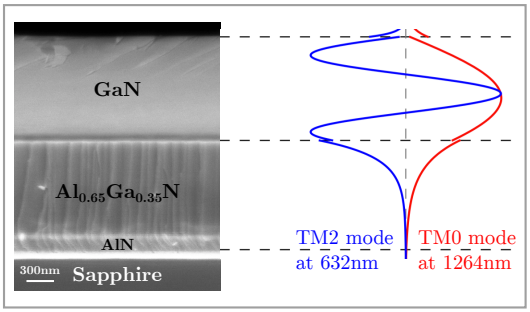

Fig. 3. A cross-sectional SEM image of the fabricated waveguide together with the electric field distributions for the TM0 mode at 1264nm and TM2 mode at 632nm wavelengths.

Our choice to grow an AlGaN optical cladding is motivated by numerous studies suggesting

Optics EXPRESS

that the direct growth of GaN on sapphire substrates is associated with high propagation losses [3,20]. A direct growth of thin (<1μm) high quality GaN layers on sapphire appears to be a challenging task due to the numerous defects generated by the lattice mismatch. Although in our approach the air/GaN/AlGaN waveguide can be mono-mode at the pump wavelength, the overall air/GaN/AlGaN/sapphire structure supports multiple higher order modes. But due to the high effective index contrast ($\Delta n > 0.1$) between the modes guided in respectively GaN and AlGaN layers we were able to selectively inject light in the modes used for non-linear interactions. While characterising the sample in the visible range using a prism coupling technique [24], we measured a small residual coupling of 2-6% to the higher order modes guided in AlGaN layer. The fact that this inter-modal coupling loss is negligible in comparison to the 10dB/cm propagation losses reported earlier [20], clearly supports our choice of an AlGaN cladding layer over the growth of GaN waveguides directly on sapphire substrates.

We optimized the GaN layer thickness and the Al content in the AlGaN cladding of the waveguide in order to reach the phase matching between TM0 and TM2 modes with the harmonic wavelength around 630nm. The electric fields distributions for the TM0 mode at 1264nm and TM2 mode at 632nm wavelengths are shown in Fig. 3. This choice of the wavelengths was particularly convenient for us, since prior to the nonlinear experiments we were able to perform a detailed linear characterisation of our waveguide at 633nm using the prism coupling technique and a He-Ne laser emitting at 633nm. We were able to measure coupling angles, effective indices and propagation losses for different modes. To estimate the propagation losses, we selectively coupled the light in a given mode and measured the decrease of the intensity of the scattered light along the propagation line. This study allowed us to discover the influence of the surface roughness on the propagation losses.

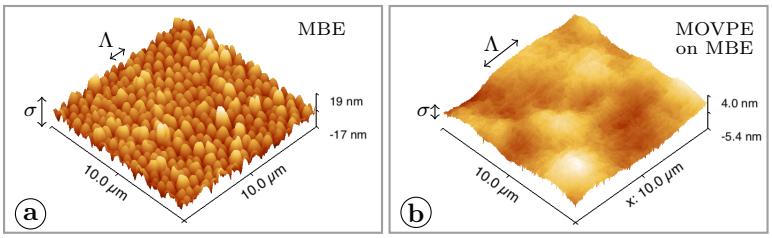

surface	rms, σ	Λ	TM0	TM1	TM2
MBE	4.3nm	0.3μm	7dB/cm	13dB/cm	16dB/cm
MOVPE on MBE	1nm	1.5μm	<1dB/cm	1dB/cm	4dB/cm

Fig. 4. (a) An AFM image of 10μm by 10μm surface area of the sample grown by MBE technique. (b) A similar AFM scan, that was done after the MBE surface was covered by a thin 60nm MOVPE layer. This regrowth made a positive impact both on the amplitude σ and the characteristic spatial scale Λ of the surface roughness. σ and Λ are determined from the exponential fit $\sigma^2 \exp(-r/\Lambda)$ of the autocorrelation function for the surfaces. The table attached to this figure summarizes the characteristics of the roughness and the values of the corresponding propagation losses at 633nm.

Initially we were using the same 1.2μm GaN/1μm AlGaN/sapphire waveguide grown by MBE but without additional MOVPE surface cover. For this waveguide we observed high propagation losses of 7-16dB/cm, see the table in Fig. 4. As we regrew a thin 60nm GaN layer by MOVPE, the surface became smoother and the propagation losses dropped to 1-4dB/cm. This study clearly shows that a relatively small surface roughness with rms=4.5nm can be responsible for high propagation losses. This result is far from being trivial since in previous studies rms=10nm [12] or rms=4nm [17] were reported as negligibly small. It should be noted that usually the surface

Optics EXPRESS

roughness for MBE-grown GaN layers is referenced as kinetic surface roughness, since it is closely related to the Ga atom mobility during the growth. The amplitude of this roughness increases with the thickness of the grown layer and the characteristic spatial frequencies of this roughness are determined by the Ga diffusion length and thus the growth temperature [25]. In our case the high spatial frequencies of MBE kinetic surface roughness with a characteristic scale of $\Lambda = 0.3\mu$m, see Fig. 4(a), were responsible for the coupling between the guided and radiation modes. Here we define Λ as a decay factor in the exponential autocorrelation function of the surface roughness $\sigma^2 \exp(-r/\Lambda)$. After MOVPE regrowth we were able to reduce the amplitude of the roughness and eliminate the high spatial frequencies as shown in Fig. 4(b). It should be noted that the same result in principle could be reached using a high temperature annealing without additional regrowth. We believe that the combination of the AlGaN cladding layer with a very smooth surface allowed us to realize low-loss GaN guiding layers.

4. SHG measurements and discussions

SHG experiments using a prism coupling set-up have already been performed in planar GaN and AlN waveguides [14, 15] with a highest reported efficiency of $0.001\%\cdot W^{-1}cm^{-2}$. Using the same set-up, we obtained a conversion efficiency of $0.15\%\cdot W^{-1}cm^{-2}$, which confirms the drastic improvement of the quality of the guiding layers.

The general scheme of our experiment is shown in Fig. 5(a). As a laser source, we use a pulsed EKSPLA NT242 OPO with 1kHz repetition rate and 4ns pulse duration. Before injection in the waveguide we focus the beam using a convex lens of 17cm focal length. Since there is no lateral confinement in the planar waveguide this step is important and it allows us to benefit from a higher power density due to the beam focalization. Using the first prism we selectively inject the pump at 1260nm in the TM0 mode. The pump propagates about 4mm in the waveguide and generates the harmonic in the TM2 mode at 630nm. The second harmonic and the pump are decoupled and separated by the second prism and sent on appropriate detectors. We used only 4mm propagation distance so that the spectral width of SHG acceptance curve, which decreases as the propagation distance increases, could be larger than the spectral width of the OPO pump.

First we used a silicon photo-diode to measure the average harmonic power as a function of the pump wavelength, see Fig. 5(b). We observe a sharp phase matching curve which is in a close agreement with the theory. We used two pyro-electric detectors to perform a pulse by pulse synchronized detection of the harmonic and the pump at 1263.7nm which corresponds to the maximum of the second harmonic signal in Fig. 5(b). The results of the synchronized detection are shown in Fig. 5(c). It should be noted that the variation of the pump energy between 200nJ and 350nJ was not obtained by an attenuator; this variation is due to the OPO energy fluctuations from pulse to pulse. These laser fluctuations may also explain the deviation of the experimental data from the quadratic fit in Fig. 5(c), as for a given energy the duration of the pump pulse may also fluctuate around 4ns changing the peak pump power and introducing the deviations into the harmonic signal.

For 350nJ of pump energy we collect around 7nJ of the second harmonic, meaning that the maximal energy conversion that was reached is around 2%. Using a quadratic fit for the experimental data in Fig. 5(c), and assuming a 4ns pulses duration and a 4mm interaction distance we estimate an average conversion efficiency to be $0.15\%\cdot W^{-1}cm^{-2}$.

In Table 1 we compare our results to the state of the art results obtained for different AlGaN structures, such as micro-rings, micro-disks, photonic crystals, ridge waveguides and PO-GaN planar waveguides. We believe that in our case the low propagation losses were an essential factor for the high conversion efficiency. The same conclusion can be driven for the AlN micro-rings with a relatively low nonlinear coefficient 1 pm / V but with very high quality factors Q=230 000 corresponding to 1.5dB/cm losses at 1550nm.

The results of the theoretical modelling presented in Fig. 2(d) suggest that the obtained

Optics EXPRESS

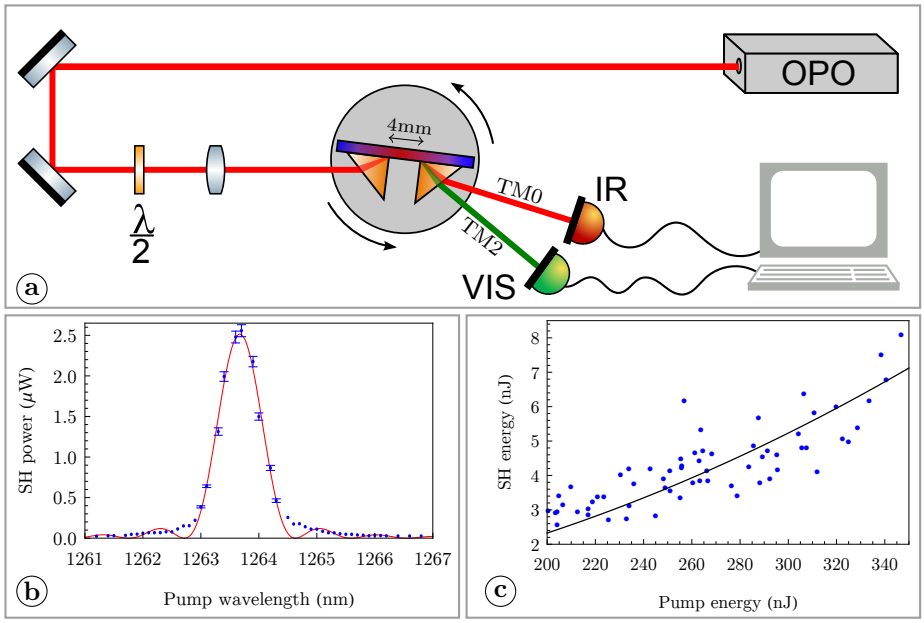

Fig. 5. (a) A general scheme of our SHG experiment. (b) The average harmonic power measured as a function of the pump wavelength using a silicon photo-diode; the red curve represents the experimental data fit with the square of the sinc function. (c) SH pulse energies as a function of the pump pulse energies; the black curve represents the quadratic fit of the experimental data. Results in the (c) were obtained by a synchronized pulse-by-pulse detection of the SH and the pump with pyro-electric detectors.

Table 1. Summary of best reported efficiencies of second harmonic generation for different AlGaN based guiding structures.

Ref.	Structure	pump wavelength	pump laser	max. power conversion	efficiency
[18]	AlN μ-ring	1550nm	cont., P_{max}=27mW	12%	2.5%·mW^{-1}
this work	GaN planar waveguide	1260nm	pulsed, 4ns, 1kHz P_{peak}=90W	2%	0.15 %·W^{-1}cm^{-2}
[13]	PO-GaN	1600nm	pulsed, 130fs, 80MHz P_{peak}=670W	0.1%	$1.2 \cdot 10^{-4}$ %·W^{-1}cm^{-2}
[7]	GaN PhC	1550nm	cont., P_{max}=0.78mW	$2 \cdot 10^{-4}$%	$2.4 \cdot 10^{-4}$ %·mW^{-1}
[26]	AlN ridge	1550nm	cont., P_{max}=50mW	$0.3 \cdot 10^{-4}$%	$0.7 \cdot 10^{-5}$ %·mW^{-1}
[16]	GaN μ-disk	1500nm	cont., P_{max}=1.1mW	$2 \cdot 10^{-7}$%	$2 \cdot 10^{-7}$ %·mW^{-1}

efficiency of 0.15%·W^{-1}cm^{-2} can be further improved. The first step would be a fabrication of ridge waveguides from the high quality planar guiding layers. The ridge waveguides would allow to obtain higher lateral confinements and to reach 10%·W^{-1}cm^{-2} conversion efficiencies. The main challenge in this case is to preserve the same low propagation losses that were observed for the planar waveguides. Low propagation losses of 1.5dB/cm at 1550nm have been already demonstrated for AlN micro-rings [18]. An additional advantage of our approach is that in our

Optics EXPRESS

case the waveguide width acts as a free parameter in a few micron range. This can allow the fabrication of few micron wide waveguides that are less sensitive to the side walls roughness and still suitable for modal phase matching. The next step of the efficiency improvement would require some kind of polarity inversion. One solution is the planar polarity inversion combined with modal phase matching; this approach could allow $100\%\cdot W^{-1}cm^{-2}$ conversion efficiencies. Another solution is to use periodically oriented GaN (PO-GaN) structures that may allow $1000\%\cdot W^{-1}cm^{-2}$ conversion efficiencies. Previous studies have shown that PO-GaN structures have a major defect of macroscopic surface roughness which is not compatible with low propagation losses. In the meantime the structures with planar polarity inversion may allow to eliminate the problem of the surface roughness and still propose high conversion efficiencies reaching $100\%\cdot W^{-1}cm^{-2}$.

5. Conclusion

In this article we presented a new GaN/AlGaN platform for non-linear optics. Our study demonstrates that this platform can simultaneously provide a high tunability, low propagation losses and high conversion efficiencies. The broadband character of this platform is confirmed by the fact that TM0/TM2 interactions allow power conversion between the near-infrared and the visible spectral regions, while TM0/TM1 interactions allow the conversion from mid-infrared to near-infrared spectral regions. We propose a new way towards high conversion frequencies based on modal phase matching with improved overlaps due to planar polarity inversion. This approach can provide conversion efficiencies up to $100\%\cdot W^{-1}cm^{-2}$ in channel waveguides and may become a viable alternative to periodically oriented GaN structures. At the first stage we have confirmed that indeed by combining proper AlGaN cladding layers together with a very smooth surface it is possible to fabricate high quality GaN guiding layers. For these layers we have observed low propagation losses going below 1dB/cm at 633nm and have reached 2% power conversion from the near-infrared to the visible spectral region with an efficiency of $0.15\%\cdot W^{-1}cm^{-2}$. In future studies we will fabricate ridge waveguides in order to get higher power densities. We will also realize planar polarity inversion in order to improve the modal overlaps and SHG conversion efficiencies.

Funding

Agence nationale de la recherche (ANR): GANEX (ANR-11-LABX-0014) and NANOGANUV (ANR-14-CE26-0025-01).